Regulation of Actin Polymerization in Cell-free Systems by GTPγS and Cdc42

Sally H. Zigmond,* Michael Joyce,* Jane Borleis,§ Gary M. Bokoch‡ and Peter N. Devreotes§

*Biology Department, University of Pennsylvania, Philadelphia, Pennsylvania 19104-6018; ‡Department of Immunology and Department of Cell Biology, The Scripps Research Institute, La Jolla, California 92037; and §Department of Biological Chemistry, The Johns Hopkins School of Medicine, Baltimore, Maryland 21205

Abstract. We have established a cell-free system to investigate pathways that regulate actin polymerization. Addition of GTPγS to lysates of polymorphonuclear leukocytes (PMNs) or *Dictyostelium discoideum* amoeba induced formation of filamentous actin. The GTPγS appeared to act via a small G-protein, since it was active in lysates of *D. discoideum* mutants missing either the α_2- or β-subunit of the heterotrimeric G-protein required for chemoattractant-induced actin polymerization in living cells. Furthermore, recombinant Cdc42, but not Rho or Rac, induced polymerization in the cell-free system. The Cdc42-induced increase in filamentous actin required GTPγS binding and was inhibited by a fragment of the enzyme PAK1 that binds Cdc42.

In a high speed supernatant, GTPγS alone was ineffective, but GTPγS-loaded Cdc42 induced actin polymerization, suggesting that the response was limited by guanine nucleotide exchange. Stimulating exchange by chelating magnesium, by adding acidic phospholipids, or by adding the exchange factors Cdc24 or Dbl restored the ability of GTPγS to induce polymerization. The stimulation of actin polymerization did not correlate with PIP_2 synthesis.

CHEMOATTRACTANT stimulation of actin polymerization is a highly conserved process intimately involved with induced pseudopod extension. Stimulation of either polymorphonuclear leukocytes (PMNs)[1] or *Dictyostelium discoideum* amoeba causes a twofold increase in filamentous (F)-actin level (McRobbie and Newell, 1983; Devreotes and Zigmond, 1988). This large F-actin change makes these cells useful for studies of actin polymerization. While chemotaxis induced by growth factors appears to use tyrosine kinase-linked receptors, chemoattractant-induced polymerization in both PMNs and *D. discoideum* amoeba requires activation of a heterotrimeric G-protein by a seven transmembrane domain receptor. Chemotaxis is blocked by pertussis toxin in PMNs and by deletion of either the appropriate Gα or the unique Gβ subunit of the heterotrimeric G-protein in *D. discoideum* (Newell et al., 1990; see Results). Chemoattractant plus GTP or GTPγS alone can stimulate polymerization in permeabilized PMNs (Downey et al., 1989; Therrien and Naccache, 1989; Bengtsson et al., 1990; Redmond et al., 1994; Tardif et al., 1995). In permeabilized PMNs, pertussis toxin blocks the actin polymerization induced by chemoattractant plus GTP but does not block the GTPγS-mediated response. It is possible that GTPγS stimulates actin polymerization via direct activation of a downstream small G-protein. This could imply that the heterotrimeric G-proteins signal to the small G-proteins during chemoattractant stimulation of actin polymerization in vivo. Chemoattractants do stimulate translocation of Cdc42 as well as Rac and Rho from the cytoplasm to the membrane fraction of PMNs and stimulate guanine nucleotide exchange on Rho in L1/2 B lymphocyte cell line (Bokoch et al., 1994; Phillips et al., 1995; Laudanna et al., 1996). Otherwise, little is known regarding the involvement of small G-proteins in chemoattractant-induced actin polymerization in neutrophils or in *D. discoideum.*

Small G-proteins of the Rho family, including Cdc42, Rac, and Rho, affect actin levels and organization in a number of cell types. In Swiss 3T3 cells, different members of the Rho family affect specific patterns of actin organization (Nobes and Hall, 1995; Nobes et al., 1995). Thus, injection of constitutively active Cdc42 induces filopodia; constitutively active Rac induces lamellipodia, and constitutively active Rho induces stress fibers. Changes in F-actin organization induced in these cells by growth factors can be blocked by dominant-negative mutants of the Rho fam-

Please address all correspondence to Sally Zigmond, Biology Department, University of Pennsylvania, Philadelphia, PA 19104-6018. Tel.: (215) 898-4559; Fax: (215) 898-8780.

1. *Abbreviations used in this paper*: F-actin, filamentous actin; G-actin; globular actin; GDI, guanine nucleotide dissociation inhibitory factor; GEF, guanine nucleotide exchange factor; GST, glutathione-S-transferase; HSS, high speed supernatant; LSS, low speed supernatant; PI, phosphatidylinositol; PIP_2, phosphatidylinositol bisphosphate; PMN, polymorphonuclear leukocytes.

ily. Rho family members also affect actin changes in cells widely separated in evolution including actin assembly at new bud sites in *Saccharomyces cerevesie* (Li et al., 1995) and in extending neurites and hairs in *Drosophila* (Luo et al., 1994; Eaton et al., 1996). In permeabilized platelets, recombinant Rac increases the availability of actin filament barbed ends (Hartwig et al., 1995). Rho family members also affect cell functions other than actin arrangements including superoxide production, cell division, and gene expression (Bokoch, 1994; Reif et al., 1996).

In spite of rapid increases in knowledge of the Rho family, many questions remain unanswered. The molecular pathway between growth factor receptors and downstream Rho family members, by analogy with Ras, is often assumed to occur through regulation of their guanine nucleotide exchange factors (GEFs). However, in most cases such regulation remains to be defined. The molecular pathway downstream of the Rho family that mediates the F-actin changes are just beginning to emerge. In several cell types, Rho stimulation of stress fiber formation may be mediated through regulation of myosin phosphorylation (Chrzanowska-Wodnicka and Burridge, 1996; Kimura and Ito, 1996). Proposed downstream mediators of Rac and Cdc42 include PAK, WASP, IQGAP, and POR1 (Rac only) (Burbelo et al., 1995; Hart et al., 1996; McCallum et al., 1996; VanAeist et al., 1996; Sells et al., 1997). However, mutants in Rac and Cdc42 with decreased ability to bind PAK and WASP still mediate F-actin rearrangements, suggesting that these interactions are not essential (Joneson et al., 1996; Lamarche et al., 1996). In permeabilized platelets, Rac stimulation of phosphatidylinositol bisphosphate (PIP_2) synthesis has been implicated in the F-actin changes, since PIP_2 is known to uncap filaments in vitro (Hartwig et al., 1995; Schafer and Coopers, 1995; Barkalow et al., 1996). However, PIP_2 affects many processes, and its role in regulation of actin polymerization in vivo requires further study.

To study these pathways, it is essential to have a system that responds to intermediates in the signaling pathway and that is stable enough to allow manipulation. Studies of actin polymerization in intact cells are limited because it is difficult to alter the relevant components quantitatively and acutely. Studies in permeabilized cells are limited by the fact that pores large enough to allow extracellular protein to enter the cell also allow globular (G)-actin to rapidly leave the cell (Redmond et al., 1994). In this paper we characterize the ability of GTPγS to induce actin polymerization in lysates of neutrophils and *D. discoideum* amoeba.

Materials and Methods

Lysates of PMNs

Rabbit peritoneal exudate PMNs, obtained as described previously, were suspended at 3–6 × 10^8 cells/ml in saline and incubated with 1 mM di-isopropylfluorophosphate (DFP; 1/1000 dilution of 1 M stock; Sigma Chemical Co., St. Louis, MO), for 5 min on ice. The cells were washed two times with cold saline and resuspended at 3 × 10^8 cells/ml in intracellular physiological buffer IP: 135 mM KCl, 10 mM NaCl, 2 mM $MgCl_2$, 2 mM EGTA, 10 mM Hepes, pH 7.1). Protease inhibitors (1 μg/ml leupeptin, 1 μg/ml benzamidine, 10 μg/ml aprotinin, 10 μg/ml Tame) were added, and the cells were incubated in a Parr bomb at 350 lb/in^2 for 15 min on ice. Upon release of pressure, the lysate was used immediately or stored on ice as described.

Lysate of D. discoideum Amoeba

Cells were grown in HL-5 based media as previously described (Devreotes et al., 1987). Amoeba were starved at 2 × 10^7 cells/ml and stimulated at 6-min intervals with 50 nM cAMP for 5 h. Cells were diluted to 1 × 10^7 cells/ml and shaken at 200 rpm with 3 mM caffeine for 15 min. Cells were spun and resuspended with cold PM (10 mM PO_4 buffer, pH 6.1, and 2 mM $MgSO_4$) at 5 × 10^7 cells/ml for intact cell stimulations and at 3 × 10^8 cells/ml for preparation of lysates. At time of lysis, cells were mixed 1:1 with PM containing with 20 mM KCl and 1 mM EGTA and lysed by passage through a 5-μm pore size filter.

D. discoideum Mutants

D. discoideum mutants were constructed by targeted gene disruption. Mutants lacking the $G\alpha_2$ (myc2) and Gβ (LW6 and LW14) subunits have been described previously (Chen et al., 1994; Wu et al., 1995). Controls used in the experiments reported here were the wild-type AX-3 strain.

Low and High Speed Supernatants

The low speed supernatant (LSS) was the supernatant of lysate spun at 4°C at 14,000 rpm for 5 min (in microfuge) ~1.5 × 10^5 *g* min. The high speed supernatant (HSS) was made from LSS by spinning at 80,000 rpm for 20 min (~5.6 × 10^6 *g* min) in Beckman TL 100 centrifuge using a 100.1 (*D. Discoideum*) or a 100.2 or 100.3 rotor (PMN). When the HSS was diluted into TRITC–phalloidin (see below) and pelleted again, the amount of TRITC–phalloidin present in the pellet was 10–20% of that in the lysate. The number of nucleation sites assayed by the rate of pyrenyl actin polymerization (see below) was ~10% of those present in the lysate. HSS could be frozen at −80°C for at least 6 mo with full retention of GTPγS sensitivity.

F-Actin Determination

F-actin was quantified from TRITC–phalloidin staining of pelleted material, modified slightly from the original description (Howard and Oresajo, 1985). Aliquots of lysates or supernatants were incubated unless stated otherwise at equivalent of 1.5 × 10^8 cells/ml at 37°C for PMNs or at room temperature for *D. discoideum.* Reactions were stopped by dilution of aliquots (usually between 30 and 60 μl) into 860 μl IP buffer containing 0.4 μM TRITC–phalloidin (Sigma Chemical Co.) and 0.1% Triton. After staining for 1 h, the samples were spun at 80,000 rpm for 20 min in an ultracentrifuge at high speed (TL100; Beckman Instr., Fullerton, CA) or for 5 min at 14,000 in the microfuge (low speed). The pellets were extracted with 1 ml of methanol, and after ~20 h the fluorescence (540 ex/575 em) was read. To determine nonsaturable staining, 4 μM unlabeled phallacidin was included.

Pyrenyl actin assays of sites that nucleate polymerization were performed as described previously (Cano et al., 1991).

Reagents

Recombinant Proteins. Recombinant Rac1 and Cdc42 were expressed in a baculovirus insect cell expression system as described (Heyworth et al., 1993; Xu et al., 1994). The Cdc42 was a glutathione-S-transferase (GST) construct and was isolated on GST beads, as per *E. coli* proteins, except from a membrane detergent lysate (to obtain the isoprenylated protein only). The amounts of proteins used in the assays were based on activity of the small GTPase proteins as determined by their ability to bind [^{35}S]GTPγS. The original GST–Cdc42 construct was a gift from Dr. R. Cerione (Cornell University, Ithaca, NY). The purified G-proteins were charged with GTPγS by incubating for 10 min at 30°C with 100 mM GTPγS in EDTA/Mg to give a final Mg concentration between 100 and 1,000 nM (Knaus et al., 1992). The Mg concentration was then increased to 2 mM in excess of the EDTA present, and the samples were stored on ice until use. G12V Cdc42 expressed in *E. coli* was a gift of Dr. J. Meinkoth (University of Pennsylvania Medical School, Philadelphia, PA). The G12V Cdc42 was tested with and without precharging with GTPγS. This protein did induce filopodia when injected into cells (Meinkoth, J., personal communication).

The PAK1 fragment that binds both Rac and Cdc42 is composed of amino acids 65–150 from human PAK1 (Manser et al., 1994). Recombinant Cdc24 and Dbl were expressed in baculovirus and generously provided by Drs. R. Cerione, J. Glaven, and T. Nomanbhoy (Cornell Univer-

sity). For experiments with both the PAK fragment and Cdc24, the supernatants were incubated for 5 min at room temperature with the recombinant proteins before warming to 37°C for 10 min.

The anti-PIP_2 antibody was obtained from PerSeptive Biosystems (Framingham, MA). PIP and PIP_2 were from Boehringer Mannheim (Indianapolis, IN); diacylglycerol (DiC_8) was obtained from Molecular Probes (Eugene, OR); brain extract (Type I: folch fraction I from bovine brain), and all other chemicals, unless noted, were obtained from Sigma Chemical Co.

Liposomes. Liposomes and/or micelles were created by resuspending various dried lipids to 10 mg/ml in 0.1 M Tris, pH 7.5, and sonicating on ice 8 cycles of 5 s on and 10 s off at level 40 on a sonic demembranator (Model 150; Dynatech Labs, Chantilly, VA). Samples were then diluted into IP buffer and mixed with HSS for F-actin assays.

Negative Staining of Actin Filaments

HSS were incubated for various times with buffer or Cdc42-GTPγS before an EM grid was placed on a drop of the solution. The grid was washed on two water drops and then placed on a drop of 1% uranyl acetate, drained, and dried. The samples were viewed at magnifications between 15,000 and 50,000.

Fluorescence Microscopy

Samples were incubated in a tube and then stained with TRITC–phalloidin and observed in the microscope with a 100× objective. Other samples were allowed to polymerize in the presence of phalloidin in a sealed slide coverslip preparation for 5 min at 37°C before observing. Similar results were observed with both methods, although there was more clumping of filaments when they were transferred from tube to slide after polymerization. In most cases, glucose, glucose oxidase, and catalase were included to reduce quenching during observation and photography. Photographs were taken on TMAX 400 and processed with classical darkroom methods.

Actin Analysis by SDS Gels

Samples were prepared as for F-actin determinations but diluted only twofold into TRITC–phalloidin (0.8 μM) and pelleted in the microfuge (14,000 for 5 min) within 10 min. The pellets were suspended in sample buffer and run on 10% polyacrylamide–SDS gels. The Coomassie blue staining band migrating at 43,000 was quantified by scanning in a densitometer and compared to a standard curve of G-actin processed similarly.

PIP_2 Synthesis

PIP_2 synthesis was performed with minor modification as described (Moritz et al., 1992). The PIP/PS micelles to be used as substrate were formed from dried lipid (0.16 μmol of total phospholipid; 80 nmol each), resuspended in 0.6 ml of micelle buffer (50 mM Tris-HCL, pH 7.4, 0.33 M sucrose, 0.133% PEG 20,000, 150 mM NaCl, BSA 0.67 mg/ml), and sonicated for 3 min on ice at 50 W output, 5 s on and 10 sec off.

For each assay of PIP_2 synthesis, a 50 μl sample contained HSS of 3×10^7 cell equivalents/ml in 50 mM Tris-HCl, pH 7.4, 100 mM NaCl, 15 mM $MgCl_2$, 1 mM EGTA, 80 μM PIP, 80 μM PS, BSA (0.4 mg/ml), 0.25 M sucrose, 0.1% PEG 20,000, 0.04% Triton X-100, 50 μM ATP, with 1–2 Ci/mmol [^{32}P]g-ATP (Amersham, Arlington Heights, IL). Samples were incubated for 5 min with no addition or with 100 μM GTPγS or with 100 nM Rac or Cdc42 charged with GTPγS.

The reaction was stopped by adding 188 μl ice-cold mix ($CHCl_3$/MeOH/1 N HCl [12/30/3 vol/vol/vol]) and vortexing well. Carrier lipids (5–10 μg of brain lipids) were added to each tube. Then 25 μl of 1 N HCl and 150 μl of $CHCl_3$ were added and vortexed. Samples were spun 2 min in microfuge to split phases. The lower $CHCl_3$ phase was removed to a new polypropylene tube. After addition of 150 μl of $CHCl_3$ to the aqueous phase, samples were vortexed again, spun, and the lower $CHCl_3$ phase removed and combined with the previously separated $CHCl_3$ phase. The combined $CHCl_3$ phases were then washed once with an equal volume of water. Samples were spun for 2 min, and 200 μl of the $CHCl_3$ phase was removed, dried in a speed vac, resuspended in 15 μl of $CHCl_3$/MeOH, and spotted on grooved lanes on a silica gel plate (60A; Whatman, Clifton, NJ). After drying, another 15 μl was added to the tube and respotted on the plate. The TLC plate had been prepared the same day by dipping three times in potassium oxalate solution and then, after drying at room temperature, heating at 85°C for 60 min to dry. Standards of PIP and PIP_2 were also spotted (20 μL of 2 mg/ml in MeOH/$CHCl_3$) and later detected with I_2. Plates were run in tank with solvent (MeOH/$CHCl_3$/H_2O/NH_3, 100/70/25/15). Radioactive spots were quantified on screens of a Phosphoimager (Molecular Dynamics, Sunnyvale, CA).

Results

GTPγS Induces Actin Polymerization in Cell Lysates

GTPγS addition to lysates of either PMNs or *D. discoideum* amoeba induced actin polymerization. The F-actin increase was optimal when the lysate concentration was 1.5×10^8 cell equivalents/ml, an ~10-fold dilution of intact cell cytoplasm (Fig. 1 *A*). At this concentration, GTPγS typically caused a twofold increase in TRITC–phalloidin staining. This is similar to the increase caused by chemoattractants in intact cells. At lower concentrations, the extent of polymerization is decreased presumably because of dilution of the cytoplasmic components, including the reservoir of sequestered G-actin that is used for polymerization (Tardif et al., 1995). At higher lysate concentrations, the response was limited by a precipitation that occurred during warming of the lysate. The maximal GTPγS-induced F-actin increase was complete in ~5 min (Fig. 1 *B*). Maximal F-actin levels were induced with concentrations of GTPγS ≥30 μM (Fig. 1 *C*). The response was specific to GTPγS as 100 μM ATPγS induced only a slow increase in F-actin, reaching, after 20 min, about half of the increase induced by 100 μM GTPγS in 3 min. The presence of GTPβS, 100 μM or 1 mM, inhibited the F-actin induced by 100 μM GTPγS by 36 and 58%, respectively. Neither GTP nor chemoattractant plus GTP induced an increase in F-actin. The behavior of amoeba lysates assayed at 22° (not shown) paralleled those of neutrophil lysates at 37°C (Fig. 1).

The formation of actin filaments in response to GTPγS was also observed in a LSS of the lysate. Since most of the F-actin in the lysate is removed at low speed, the increases in F-actin levels relative to basal levels were greater in the LSS; however, the absolute change in TRITC–phalloidin staining was similar, indicating that a similar amount of actin polymerized. The large fractional increase allowed us to examine the increase in F-actin morphologically. The filaments, when stained with TRITC–phalloidin, could be observed in the fluorescent microscope. In the presence of GTPγS there were many filaments which often clustered into bundles and meshworks; without GTPγS, few filaments were seen (Fig. 1, *D* and *E*).

Heterotrimeric G-Protein α- and β-subunits Were Not Required for GTPγS Stimulation of Actin Polymerization

D. discoideum mutants lacking heterotrimeric G-protein subunits were tested in vivo and in vitro for actin polymerization responses. Amoebae lacking the α subunit, $G\alpha_2$, do not exhibit chemotaxis to the chemoattractant cAMP, and mutants lacking the β subunit fail completely to move towards any chemoattractant. These defects parallel deficiencies in actin polymerization (Fig. 2 *a*, and other data not shown). In the $G\alpha_2$ null cells, cAMP does not induce actin polymerization; in the Gβ null cells, no chemoattractants trigger a response. Nevertheless, in lysates of either

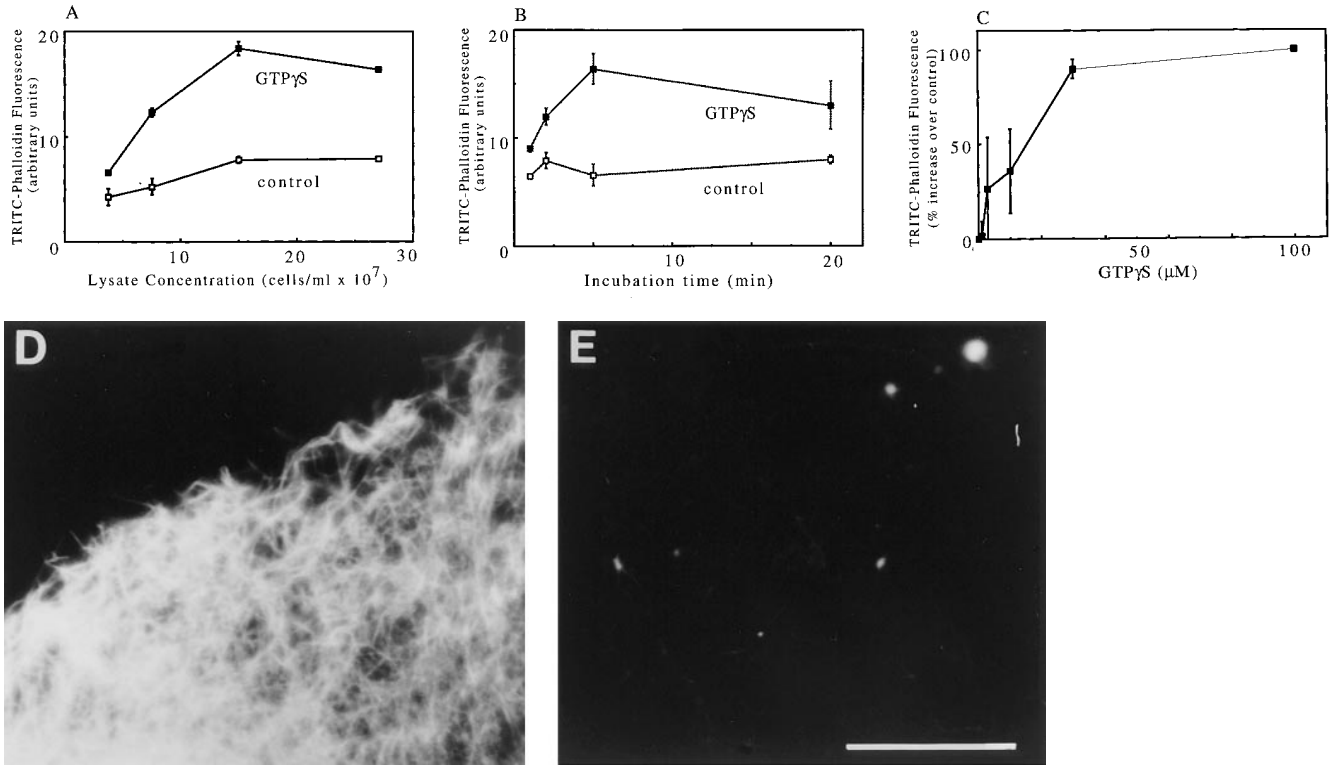

Figure 1. (*A*) Actin polymerization as function of lysate concentration in cell equivalents/ml. PMNs were bombed at 3×10^8 cells/ml; the lysate was diluted to concentrations of 28, 15, 8, and 4×10^7 cell equivalents/ml and warmed for 6 min with (*closed squares*) or without (*open squares*) 100 μM GTPγS. The samples were then diluted ~17-fold into TRITC–phalloidin, stained for 1 h before spinning at 80,000 rpm for 20 min in a tabletop ultracentrifuge (Beckman). The TRITC–phalloidin in the pellet (6×10^6 cell equivalents/pellet) was extracted with MeOH overnight and the fluorescence read at ex = 540 nm; em = 575 nm. Data presented are duplicates of an experiment (error bars are the individual values) representative of three experiments. (*B*) Time course of actin polymerization in lysate. PMN lysates at 3×10^8 cell equivalents/ml were warmed for various times with (*closed squares*) or without (*open squares*) 100 μM GTPγS before processing as described in *A*. The experimental data are the means of four experiments (with up to seven individual values). (*C*) Concentration dependence of GTPγS. PMN lysates at 3×10^8 cell equivalents/ml were warmed for 3 to 5 min in various concentrations of GTPγS and then processed as described in *A*. Data are means ±SEM compiled from at least four experiments: $n = 4$ (1 μM), 5 (3 μM), 7 (10 μM), 5 (30 μM), and 7 (100 μM) normalized relative to the unstimulated control. (*D* and *E*) Actin filaments induced by GTPγS and stained with TRITC–phalloidin. LSS of neutrophil lysates were incubated at room temperature for 5 min with 100 μM GTPγS (*D*) or without GTPγS (*E*) and then stained with TRITC–phalloidin and observed in a fluorescent microscope. Bar, 10 μm.

mutant, GTPγS stimulated actin polymerization (Fig. 2 *b*). The response was similar to that in wild-type cells. These observations suggested that the target for GTPγS in lysates is not a heterotrimeric G-protein but might be a downstream small G-protein.

Cdc42 Induces Actin Polymerization

Addition of purified GTPγS-activated baculovirus-expressed human Cdc42 induced actin polymerization in lysates of both PMNs and *D. discoideum* amoeba. Further studies with PMN supernatants indicated that the rate of polymerization depended on the Cdc42 concentration (Fig. 3 *A*), while the final level of F-actin achieved was similar for concentrations ≥50 nM (50–200 nM; Fig. 3 *B*). The amount of GTPγS carried over after charging the Cdc42 caused little or no polymerization (300 nM GTPγS was present per 100 nM Cdc42 [Fig. 1 *C*]).

In vivo, agonists that increase the levels of F-actin usually also increase the filament number and the availability of free barbed ends (Cano et al., 1991). Thus it was important to determine if the increase in polymerized actin observed in this in vitro assay also correlated with an increase in free barbed ends. Lysates were warmed with buffer, Cdc42, or GTPγS, and then diluted into pyrene-labeled actin; and the rate of pyrenyl actin polymerization was followed by the increase in pyrene fluorescence. Both GTPγS and Cdc42 induced an approximately twofold increase in the rate of polyme365368rization (Fig. 3 *C*). This increase in rate of polymerization was inhibited by 2 μM cytochalasin b (not shown), indicating that the elongation was occurring at the barbed ends of filaments.

The responses in this assay required appropriately processed Cdc42. Other members of the Rho family of small GTPases, Rac1 or Rho, expressed in baculovirus and charged with GTPγS did not stimulate actin polymerization in PMN lysates. The activated Rac was shown to be effective in assays of PIP_2 synthesis (see below). Cdc42 expressed in *E. coli* did not increase F-actin levels, suggesting that a specific modification such as geranylgeranylation was important for activity (Fig. 4 *A*; Heyworth et al., 1993). The activity of Cdc42 may also be enhanced by

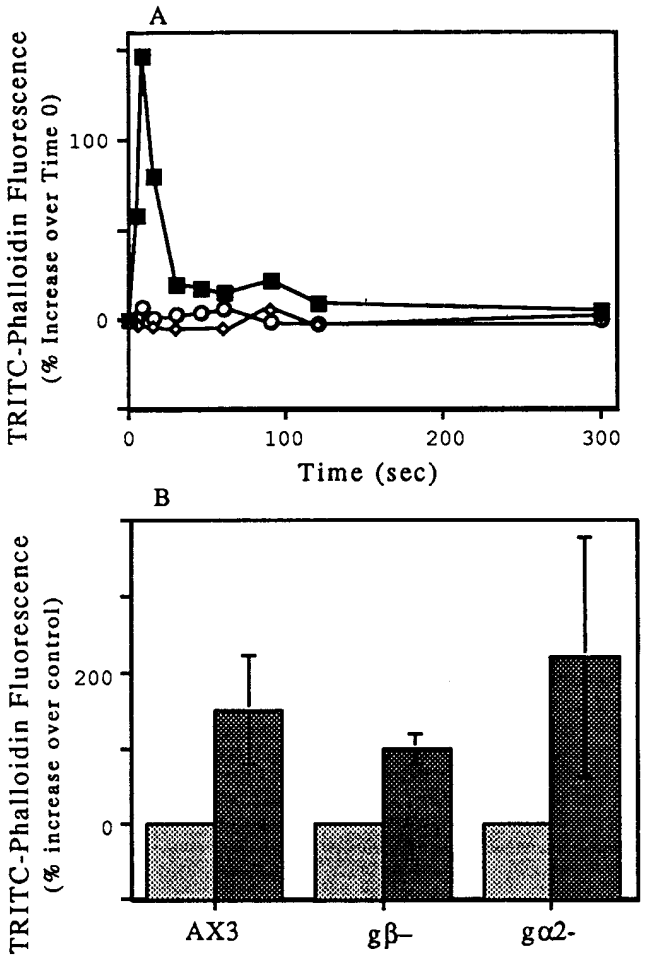

Figure 2. F-actin responses of *D. discoideum* mutants lacking the β or α2 subunits of the trimeric G-protein, $G\alpha_2$. (*A*) The F-actin in intact cells was determined by TRITC–phalloidin staining of amoeba fixed at various times after stimulation with 2 nM cAMP. Cell lines tested were wild type, AX3 (*closed squares*); Gβ− minus, LW14 (*open diamonds*); and $G\alpha_{2^-}$, JM1 (*open circles*). The data were normalized relative to the F-actin level at t = 0. (*B*) Lysates from wild type and mutants stimulated with GTPγS. Lysates of cell lines tested in *A* were stimulated with 100 μM GTPγS, and the F-actin level present was determined as described in Materials and Methods. The F-actin level in each extract without GTPγS was used to normalize the data (*grey bars*). The mean GTPγS-induced F-actin (*dark bars*) and standard deviation (*error bars*) is shown for 8 experiments with AX3, 3 experiments with LW14 ($G\beta-$) and 11 experiments with JM1 ($G\alpha_{2^-}$). Data for cells stimulated for 2 through 10 min were pooled for this figure, since separate experiments showed the F-actin levels were maximal after about 2 min and were maintained for at least 10 min.

some aggregation. In preliminary experiments, centrifugation of the activated Cdc42 preparation at 80,000 rpm for 20 min, pelleted between 15 and 50% of the immunoreactive Cdc42 (as detected by Western blots) and ~75% of its ability to induce actin polymerization (data not shown).

The effects of Cdc42 were specific. The activity required activation by GTPγS; Cdc42 without nucleotide or Cdc42 bound with GDP was ineffective. The effects of activated Cdc42 were blocked by a fragment of the enzyme PAK1, which contains the binding site for Cdc42 (Manser et al., 1995). Inhibition by the PAK fragment was most pronounced at early times; upon continued incubation, slow polymerization resulted in F-actin accumulation (Fig. 4 *B*). The GTPγS requirement and the inhibition by the PAK fragment indicates that the activity is not due to a contaminant in the Cdc42 preparation.

The Cdc42-induced filaments were collected on EM grids, negatively stained, and observed in the electron microscope. An HSS was used for these experiments. The filaments formed upon incubation with 100 nM Cdc42 for 5 min were present primarily as individual filaments of varying lengths up to at least 8 μm (Fig. 5 *A*); occasionally filament bundles were observed. Searches of grids made from HSS warmed for 5 min without Cdc42 revealed only an occasional filament (not shown). Similarly, TRITC–phalloidin-stained filaments were rarely seen in the HSS warmed without Cdc42 (Fig. 5 *B*). When HSS was warmed on the slide in the presence 100 nM Cdc42 and TRITC–phalloidin, many small filaments were observed (Fig. 5 *C*). These increases in filament number were consistent with the increase in barbed ends that nucleated polymerization, described above (Fig. 3 *C*). When warmed in a tube and then transferred to the slide, filament bundles and clusters were observed (the clusters presumably form during mixing; Fig. 5 *D*).

Interestingly, the GST–Cdc42 fusion protein still attached to glutathione bead could induce polymerization at the surface of the bead (Fig. 5, *E* and *G*). The ability of Cdc42-loaded beads to induce polymerization required activation by GTPγS (Fig. 5 *F*) and was blocked by the PAK GTPase binding fragment (Fig. 5 *H*). Like actin polymerization induced in vivo and in permeabilized cells, the GTPγS and Cdc42-induced polymerization was blocked by cytochalasin (data not shown).

HSS Lacks GEF Activity Needed for GTPγS to Stimulate Actin Polymerization

Both activated Cdc42 and GTPγS were able to induce actin polymerization in LSS (1.5×10^5 *g* min). However, only activated Cdc42 could induce polymerization in HSS (5.6×10^6 *g* min). The magnitude of the Cdc42-induced response in a lysate and an HSS made from that lysate was similar (Fig. 6 *A*). The ability of GTPγS to induce polymerization in HSS could be restored by addition of a small amount of lysate or resuspended pellet (Fig. 6 *B*). Addition of lysate equal to only 3% of the volume of the HSS was sufficient to allow polymerization. Increasing the amount of lysate increased the rate of polymerization.

Since GTPγS bound Cdc42-induced polymerization in the HSS, all components downstream of Cdc42 that are needed for actin polymerization must be present. The failure of GTPγS to act suggested that HSS lacks either a G-protein or a GEF needed for GTPγS to bind to a G-protein. Treatment of the pelleted material with GTPγS was not sufficient to induce polymerization upon dilution into the HSS. Rather, GTPγS had to be present after mixing the HSS with the particulate fraction (data not shown), suggesting that the G-protein is present in the supernatant and that the particulate fraction stimulates nucleotide exchange.

In PMN lysates, small G-proteins of the Rho family are found in the supernatant, while the GEFs are in a particu-

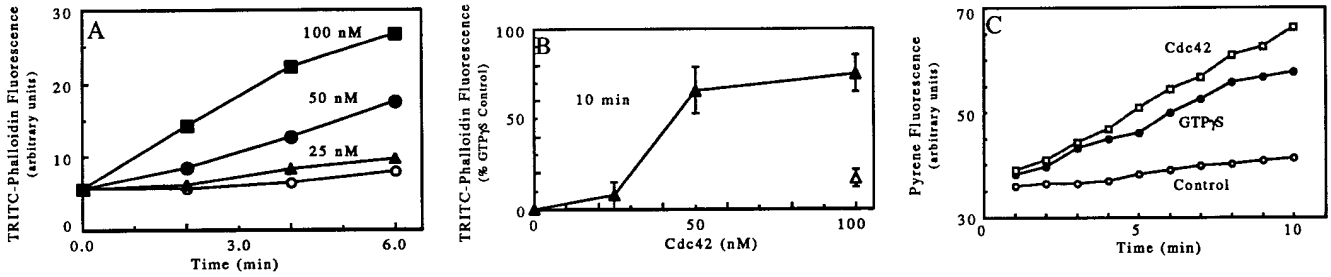

Figure 3. Recombinant Cdc42-induced actin polymerization. (*A*) Time course of polymerization as a function of Cdc42 concentration. Various concentrations of GTPγS-charged Cdc42, 0 (*open circles*), 25 (*closed triangles*), 50 (*closed circles*), or 100 nM Cdc42 (*closed squares*) were incubated with an HSS of PMN lysate for 2, 4, or 6 min before stopping with TRITC–phalloidin and processing samples. Data shown are from a single experiment representative of three. (*B*) Extent of polymerization as a function of Cdc42 concentration. Various concentrations of GTPγS-charged Cdc42 (*closed triangles*) or the GTPγS associated with 100 nM Cdc42 (*open triangle*) were incubated with the LSS of PMN lysates for 10 min. The samples were processed as described in Fig. 1 *A*. The data represent the means and SD of two experiments normalized by setting the increase in staining induced by 100 μM GTPγS to 100% (GTPγS-induced increase was 160% over basal in both experiments). (*C*) Cdc42 and GTPγs increase the rate of pyrenyl-actin polymerization. Lysates (1.5×10^8 cells/ml) were warmed for 5 min with buffer (*Control*), 100 μM GTPγS, or GTPγS-charged 100 nM Cdc42 before dilution (200-fold) into 2 mM pyrenyl-G-actin in polymerization buffer. The change in pyrene fluorescence representing polymerization of the pyrene actin was followed over time. The data shown are representative samples. In this experiment, the initial rate of polymerization (determined between 2 and 6 min) for duplicate samples was increased 2-fold by GTPγS and 2.3-fold by Cdc42.

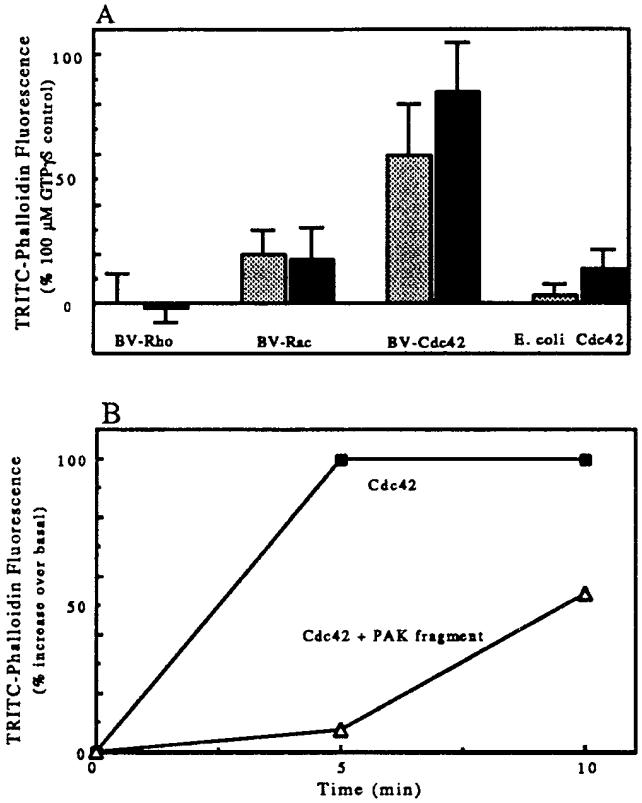

Figure 4. (*A*) The induction of actin polymerization was unique to Cdc42, other Rho family members were inactive. PMN lysates were warmed for 3 to 5 min with GTPγS-charged baculovirus-expressed Cdc42 (50 nM light bar; 100 nM dark bar); baculovirus-expressed Rho (80 nM, light bar; 200 nM, dark bar); baculovirus-expressed Rac1 (50 nM light bar; 100 dark bar); and *E. coli*-expressed ^{V12}Cdc42 (50 nM, light bar; 100 nM, dark bar). Increasing Rho or Rac to 200 nM or *E. coli*-expressed Cdc42 to 1 μM did not result in increased phalloidin staining. The samples were processed as in Fig. 1 *A*. The data represent at least two experiments with each construct. To pool data between experiments, we normalized by expressing the staining induced by a given G-protein to the increase in that experiment induced by 100 μM GTPγS (GTPγS-induced increase over basal was: mean, 97%; range, 67 to 130%, $n = 14$). Error bars represent the range of values. (*B*) The Rac and Cdc42 binding fragment of PAK inhibits actin polymerization induced by Cdc42. LSS of PMN lysates were warmed for 5 or 10 min with GTPγS-charged Cdc42 (100 nM) in the absence (*closed squares*) or presence of 1 μM PAK fragment (*open diamonds*). The samples were processed as above. The data are from one experiment, representative of three.

late fractions (Bokoch et al., 1994; Phillips et al., 1995). Thus, the possibility that the HSS was lacking guanine nucleotide exchange activity seemed likely. To test this idea we sought to supply exchange activity in various ways. First, we sought to release the G-protein from possible inhibition by guanine nucleotide dissociation inhibitory factor (GDI) by addition of phospholipids (Chuang et al., 1993; Abo et al., 1994). Addition of lamellar or micellar lipids derived from PMNs by $CHCl_3$/MeOH extraction (not shown) or commercially available extracts from brain allowed GTPγS to stimulate an increase in F-actin (Fig. 7 *A*). Liposomes of pure anionic phospholipids were also effective. The rank order effectiveness of various lipids in allowing GTPγS to induce actin polymerization was similar to that effective in displacing GDI (Chaung et al., 1993). Phosphatidylinositol (PI) the most active pure lipid tested, allowed GTPγS to induce actin polymerization when present at 15 μM. Commercially available phosphatidic acid (PA), PIP, and PIP_2 also allowed response to GTPγS when present between 50 and 200 μM. Diacylglycerol (1-oleoyl-2-acetyl glycerol) was not effective even at concentrations up to 450 μM. At the concentrations tested, most of the lipids had little effect on the F-actin level in the absence of GTPγS. However, concentrations of PI >50 μM and brain lipids and phosphatidic acid >100 μM did increase F-actin levels in the absence of GTPγS.

A second way to increase exchange of nucleotides on small G-proteins is through magnesium chelation. We che-

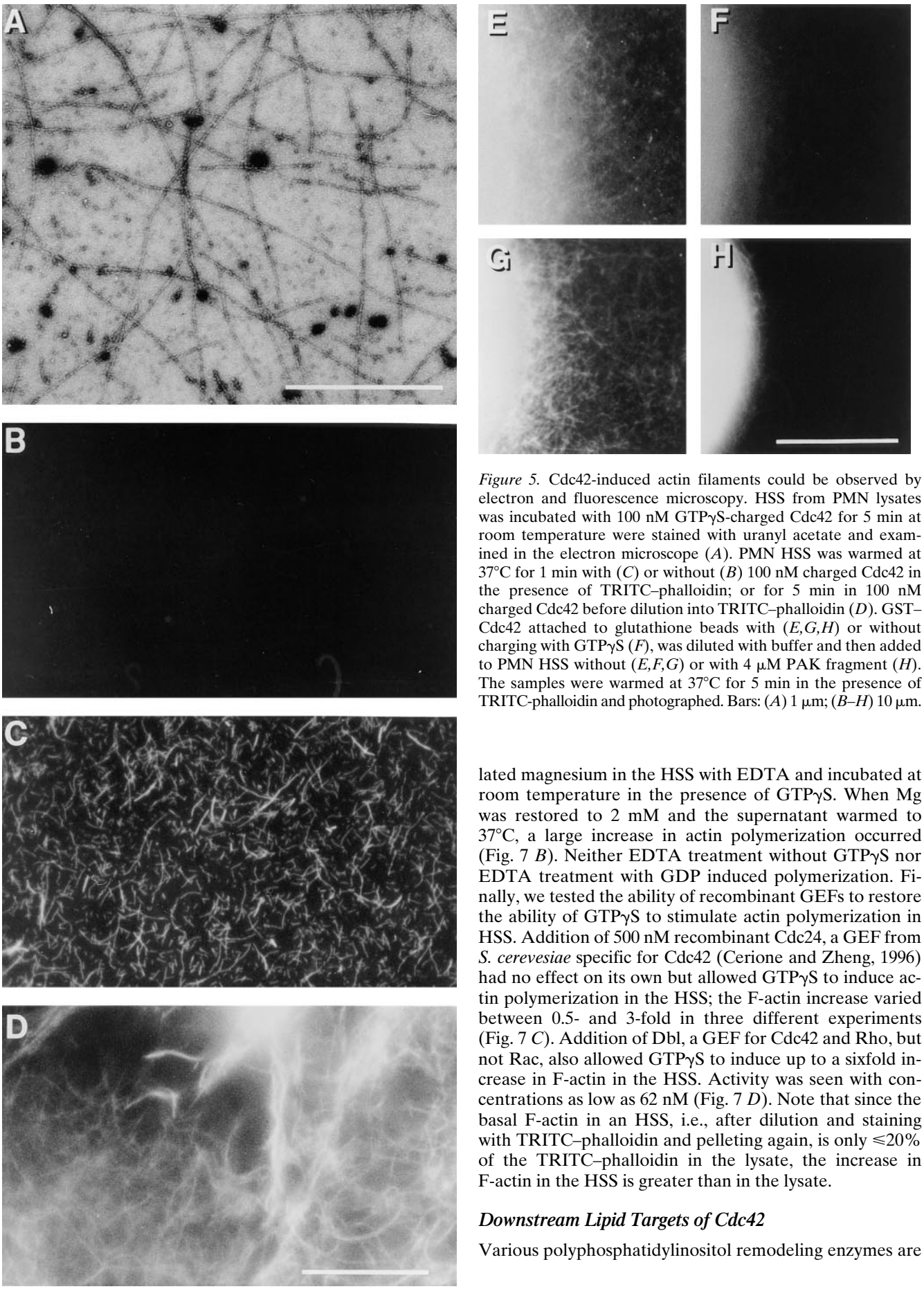

Figure 5. Cdc42-induced actin filaments could be observed by electron and fluorescence microscopy. HSS from PMN lysates was incubated with 100 nM GTPγS-charged Cdc42 for 5 min at room temperature were stained with uranyl acetate and examined in the electron microscope (*A*). PMN HSS was warmed at 37°C for 1 min with (*C*) or without (*B*) 100 nM charged Cdc42 in the presence of TRITC–phalloidin; or for 5 min in 100 nM charged Cdc42 before dilution into TRITC–phalloidin (*D*). GST–Cdc42 attached to glutathione beads with (*E,G,H*) or without charging with GTPγS (*F*), was diluted with buffer and then added to PMN HSS without (*E,F,G*) or with 4 μM PAK fragment (*H*). The samples were warmed at 37°C for 5 min in the presence of TRITC-phalloidin and photographed. Bars: (*A*) 1 μm; (*B–H*) 10 μm.

lated magnesium in the HSS with EDTA and incubated at room temperature in the presence of GTPγS. When Mg was restored to 2 mM and the supernatant warmed to 37°C, a large increase in actin polymerization occurred (Fig. 7 *B*). Neither EDTA treatment without GTPγS nor EDTA treatment with GDP induced polymerization. Finally, we tested the ability of recombinant GEFs to restore the ability of GTPγS to stimulate actin polymerization in HSS. Addition of 500 nM recombinant Cdc24, a GEF from *S. cerevesiae* specific for Cdc42 (Cerione and Zheng, 1996) had no effect on its own but allowed GTPγS to induce actin polymerization in the HSS; the F-actin increase varied between 0.5- and 3-fold in three different experiments (Fig. 7 *C*). Addition of Dbl, a GEF for Cdc42 and Rho, but not Rac, also allowed GTPγS to induce up to a sixfold increase in F-actin in the HSS. Activity was seen with concentrations as low as 62 nM (Fig. 7 *D*). Note that since the basal F-actin in an HSS, i.e., after dilution and staining with TRITC–phalloidin and pelleting again, is only ≤20% of the TRITC–phalloidin in the lysate, the increase in F-actin in the HSS is greater than in the lysate.

Downstream Lipid Targets of Cdc42

Various polyphosphatidylinositol remodeling enzymes are

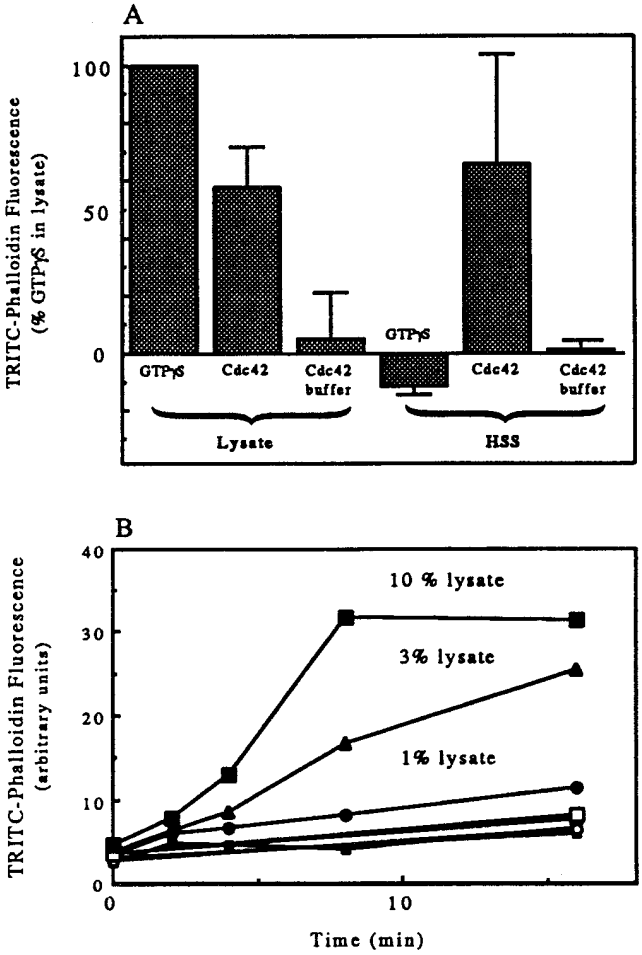

Figure 6. (*A*) Cdc42 but not GTPγS induced actin polymerization in HSS of lysates. PMN lysates were either tested directly or were used to produce a HSS: spun at 14,000 rpm for 5 min in an Eppendorf microfuge, and the supernate of this "low speed spin" was then centrifuged for 20 min at 80,000 rpm in a 100.2 rotor of a tabletop ultracentrifuge (Beckman). The lysate and supernatant of the high speed spin were warmed for 3 min (lysates) or 10 min with 100 μM GTPγS or 100 nM GTPγS-charged Cdc42 or the GTPγS carried over from activating the Cdc42 (Cdc42 buffer). Samples were then processed as described in Fig. 1 *A*. The data presented are the mean and SD of two experiments in which both lysate and HSS were tested. Data were normalized by setting the change in TRITC–phalloidin fluorescence of lysate stimulated with GTPγS as 100% (the GTPγS-induced increase over basal was 112 and 125% in the two experiments). (*B*) Addition of PMN lysate back to the HSS allowed GTPγS to induce actin polymerization. Various amounts of lysate equal to 1% (*circles*), 3% (*triangles*), or 10% (*squares*) of the volume of the HSS were incubated for various times in the presence (*closed symbols*) or absence (*open symbols*) of 100 μM GTPγS. The samples were processed as described in Materials and Methods.

potential downstream targets for Cdc42. A known target of Cdc42 is the 85-kD regulatory subunit of PI-3 kinase (Zheng et al., 1994; Tolias et al., 1995). However, addition of 100 nM wortmannin, an inhibitor of PI-3 kinase, did not inhibit the induction of actin polymerization by either Cdc42 or GTPγS (not shown). A second potential downstream target is PIP_2 synthesis, which is simulated by Rac in permeabilized platelets and has been proposed to regulate actin polymerization (Hartwig et al., 1995). We investigated whether PIP_2 synthesis was responsible for actin polymerization in PMN HSSs. In the PMN HSS, it was not possible to detect incorporation of ^{32}P from γ-labeled ATP into bands comigrating on thin layer chromatography with PIP or PIP_2. However, upon addition of substrate lipids, micelles of equimolar PS with PIP, incorporation of ^{32}P into PIP_2 was detected. Recombinant Rac stimulated synthesis of PIP_2 from PIP nearly tenfold (Fig. 8, *A* and *B*). Cdc42 stimulated PIP_2 synthesis about threefold; however GTPγS stimulated little or no synthesis of PIP_2 even when brain lipids were included to stimulate nucleotide exchange (Fig. 8, *A* and *B*). Parallel experiments run on the same day confirmed that each of these agents acted on actin polymerization as described above: Rac did not induce actin polymerization, while both Cdc42 and GTPγS (plus brain lipids) did. Thus, PIP_2 synthesis did not correlate with actin polymerization. Furthermore, as noted above, addition of PIP_2 liposomes did not stimulate actin polymerization. Finally, we tested antibodies to PIP_2 that have been effective in blocking functions of PIP_2 in some systems (Fukami et al., 1988; Gilmore and Burridges, 1996). The antibody, at concentrations effective in injection experiments, did not inhibit Cdc42-induced actin polymerization in a HSS (Fig. 8 *C*). This again suggested that PIP_2 is not needed downstream of Cdc42.

Discussion

We have developed a cell-free system that, upon stimulation with intermediates of the signal transduction pathway, exhibits an increase in F-actin. Lysates of PMN and *D. discoideum*, cells widely separated in evolution, both respond under similar conditions to GTPγS by increasing actin polymerization. The HSS is stable for several hours on ice or can be frozen and stored at −80° for several months without loss of activity. Furthermore, the lysate is amenable to fractionation and to addition of exogenous materials.

Initiation of actin polymerization in cell lysates appears to occur at the level of small G-proteins of the Rho family. Thus, addition of Cdc42 charged with GTPγS induced polymerization. Indeed, coupling between the chemoattractant receptor and actin polymerization appears lost upon lysis. The insensitivity of lysates does not reflect an uncoupling of receptor and heterotrimeric G-protein, since GTPγS regulates chemoattractant binding in lysates of both cell types (Devreotes and Zigmond, 1988). In lysates of *D. discoideum* amoeba, GTPγS stimulates adenylate cyclase, a response that depends critically on the β-subunit. Yet, in the same lysates, actin polymerization is completely independent of the presence of the β-subunit of the heterotrimeric G-protein. It seems most likely that coupling between the trimeric G-protein and downstream effectors of actin polymerization are lost upon cell lysis. It is possible that lysis itself activates guanine nucleotide exchange activity toward the downstream Rho GTPases, making regulation by trimeric G-protein redundant.

In vitro actin polymerization occurs in concentrated lysates (2- to 3-fold dilution of packed cell pellet) of various cells and oocytes (Kane, 1986; Fukami et al., 1988; Whitehead et al., 1995*a,b*). It is not clear what initiates this poly-

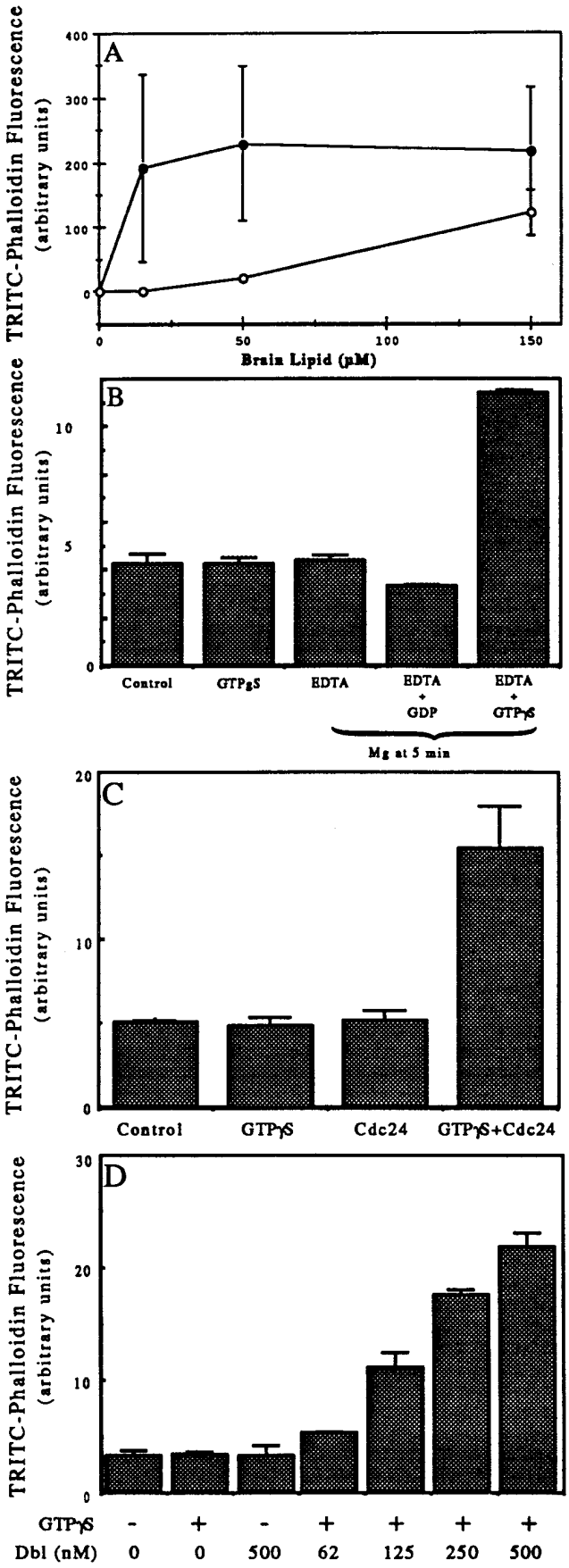

merization, which exceeds that in the cell at the time of lysis (Kane 1986). It is possible that in these concentrated extracts, activation of GEF activity upon lysis allows endogenous GTP to activate small G-proteins, which then induce actin polymerization. In the more dilute extracts used in this study, GTP is ineffective, presumably because it is hydrolyzed before it has time to act.

In the assays described here, downstream of Cdc42, all components required for actin polymerization are present in the HSS. Thus, in the HSS of both neutrophils and *D. discoideum* cells, GTPγS-charged Cdc42 could induce polymerization. However, the HSS appeared to lack the guanine nucleotide exchange activity required for GTPγS to induce polymerization. Activity in PMN HSS was restored by addition of recombinant GEFs (Cdc24 and Dbl). Our data are consistent with observations in hematopoetic cells that most of the Rac and Cdc42 are present in the supernatant (Bokoch et al., 1994; Phillips et al., 1995), while the GEFs, or factors that activate GEFs, are present in a particulate fraction (Bokoch et al., 1994; Whitehead et al., 1995*a,b*; Chardin et al., 1996).

Acidic lipids restored the ability of GTPγS to induce polymerization in the HSS, probably acting by displacement of GDI (Chuang et al., 1993). Lipids are known to facilitate guanine nucleotide exchange in several ways: (*a*) acidic lipids can displace GDI (Chuang et al., 1993). (*b*) Polyphosphatidylinositols can activate GEFs by binding to their PH domain (Chardin et al., 1996). (*c*) Polyphosphatidylinositols can also directly stimulate release of GDP from small G-proteins, including Cdc42, although since

Figure 7. (*A*) Effects of liposomes on ability of GTPγS to induce actin polymerization in HSS. HSS was incubated for 10 min at 37° without (*open circles*) or with (*closed circles*) 100 μM GTPγS and with varying concentrations of liposomes made of brain lipid. The samples were processed as described in Fig. 1. The data plotted are the means and ranges of values from duplicates of at least two experiments. (*B*) Pre-incubation of HSS with GTPγS and EDTA allowed GTPγS to stimulate actin polymerization. HSS at 1.5×10^8 cell equivalents/ml were incubated at room temperature for 5 min with no addition (*Control*), 100 μM GTPγS, 10 mM EDTA, 10 mM EDTA with 100 μM GDP, or 10 mM EDTA with 100 μM GTPγS. Then 12 mM Mg was added to each of the EDTA-containing samples; all samples were incubated for a further 5 min at 37°C. The samples were then processed as in Fig. 1 *A*. The data shown are duplicates from one experiment representative of three. (*C*) Addition of Cdc24 allowed GTPγS to stimulate actin polymerization in the HSS. HSS were incubated at room temperature for 5 min and then at 37°C for 10 min with Cdc24 buffer (*Control*); buffer plus 100 μM GTPγS (*GTPγS*); 500 nM Cdc24 (*Cdc24*); or 100 μM GTPγS and 500 nM Cdc24. The samples were processed as described in Fig. 1 *A*. The data presented are the means and ranges of duplicates of a single experiment. Similar but smaller increases (~50% increases over buffer control) were induced by Cdc24 in two additional experiments. (*D*) Addition of oncogenic Dbl allowed GTPγS to stimulate actin polymerization in the HSS. HSS were incubated at room temperature for 5 min and then 10 min at 37°C with buffer, 100 μM GTPγS, 500 nM Dbl, or with 100 μM GTPγS plus 62, 125, 250, or 500 nM oncogenic Dbl. The samples were processed as described in Fig. 1 *A*. The data presented are the means and ranges of duplicates of a single experiment. Comparable levels of stimulation were achieved by 500 nM Dbl in a second experiment.

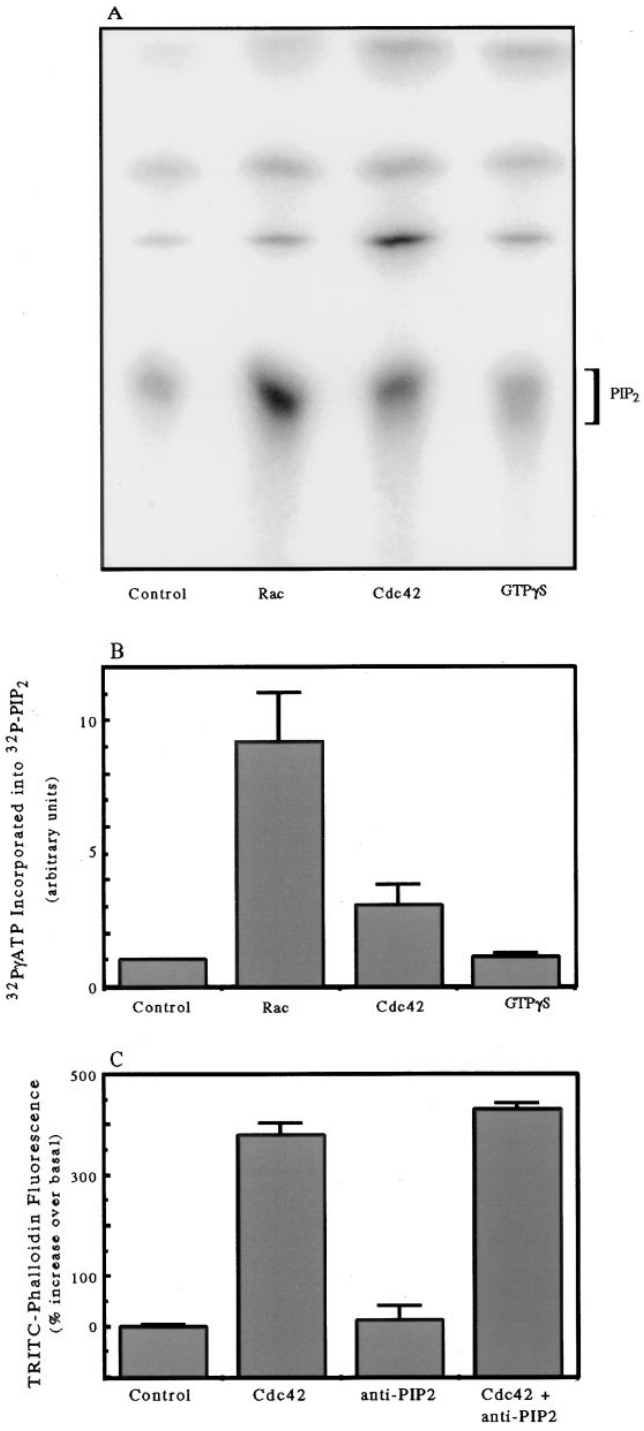

Figure 8. Stimulation of PIP_2 synthesis by GTPγS, Cdc42, and Rac. (*A*) ^{32}P incorporation into PIP_2 separated by TLC after PIP/PS micelles were mixed with HSS containing 50 μg/ml brain lipids and addition of either buffer (*Control*), 100 nM GTPγS-charged Rac, 100 nM GTPγS-charged Cdc42, or 100 μM GTPγS. The labeling and TLC were run as described in Materials and Methods. The data are representative of duplicate samples from two experiments performed on different days. (*B*) Quantitative analysis by the phosphorimager of the PIP_2 peak separated on a chromatograph as in Fig. 8 *A*. The data for each column represent the mean integrated volume value and range of values from duplicate experiments run on two separate days. (*C*) Effect of 0.2 mg/ml anti-PIP_2 antibody on Cdc42-induced actin polymerization in an HSS. The data are presented relative to the basal (control) fluorescence set at 100% and plotted as the means and ranges of duplicates from a single experiment representative of two.

GTPγS can not bind this complex, PIP_2 alone can not activate Cdc42 (Terui et al., 1994; Zhang et al., 1996). In displacement of GDI, phosphatidic acid and PI are more effective than PIs; in stimulating GEFs and releasing GDP, PIP_2 is much more effective than PI. The fact that PI was more effective than PIP or PIP_2 in allowing GTPγS to induce actin polymerization suggested that, in this system, the lipids functioned primarily through GDI displacement.

PIP_2-mediated uncapping of actin filaments has been proposed to be the downstream effector of Rac, because Rac stimulates PIP_2 synthesis (Hartwig et al., 1995; Barkalow et al., 1996; Schafer et al., 1996). However, in our system there was no correlation between PIP_2 synthesis and actin polymerization. Recombinant Rac stimulated PIP_2 synthesis, but the increase was not accompanied by increased actin polymerization. In addition, although GTPγS induced polymerization, it did not stimulate PIP_2 synthesis. That GTPγS did not stimulate PIP_2 synthesis in the HSS suggested that it did not activate endogenous Rac. This failure may be ascribed to the absence of cellular membranes, since the ability of GTPγS to activate Rac in PMN lysates depends on GEFs that pellet with the cellular membranes (Bokoch et al., 1994). Further excluding PIP_2 as a downstream mediator of actin polymerization, addition of exogenous PIP_2 did not increase F-actin level, and antibodies against PIP_2 did not block Cdc42-induced actin polymerization.

Further work will be required to determine which properties of Cdc42 are critical for its induction of actin polymerization and why Rac was ineffective. Cdc42 activity required GTPγS and some modification, probably geranylgeranylation that occurred during expression in Sf9 cells but not in *E. coli.* Activity may also be enhanced by some macromolecular organization since the Cdc42 pelleted at high speed had disproportionately high activity. Cdc42 activity in solution and attached to a bead was inhibited by the GTPase-binding fragment of PAK, which presumably acts by blocking interaction of Cdc42 with its targets.

Parallel preparations of recombinant Rac were inactive in stimulating polymerization in PMN lysate and HSS. This was surprising since Rac stimulates actin polymerization in permeabilized platelets (Hartwig et al., 1995). Perhaps, in the PMN, Rac function has been diverted to regulate the NADPH oxidase (Bokoch, 1994). Alternatively perhaps, lysis disrupts coupling of Rac to actin polymerization as it disrupts coupling of heterotrimeric G-proteins to actin polymerization.

Further work will also be required to determine whether GTPγS acts through endogenous Cdc42. Addition of the GTPase binding fragment of PAK to PMN lysates did not block GTPγS-induced actin polymerization (Joyce, M., and S.H. Zigmond, unpublished result) suggesting Cdc42 might not be the endogenous target. However, supporting endogenous Cdc42, recombinant exchange factors Cdc24 and Dbl, specific, respectively, for Cdc42 and for Cdc42 and Rho, allowed GTPγS to function in the HSS (Cerione and Zheng, 1996). The concentration of endogenous

Cdc42 in the HSS of 1.5×10^8 cells/ml was estimated by Western blots to be ~4.5 ± 2 nM (mean ±SD; Lartique, J., H. Sun, and S.H. Zigmond, unpublished observation), ~10-fold lower than the concentration of recombinant Cdc42 required to induce actin polymerization. Thus, the endogenous Cdc42 may be more active than the recombinant protein. Increased activity might result from complexes that associate endogenous Cdc42 with its downstream target. If so, the failure of the PAK fragment to inhibit the GTPγS stimulation might also be explained: this fragment might bind too slowly to compete under these conditions.

In summary, the ability to induce actin polymerization in vitro allows dissection of the pathways involved in this important process. Using this assay, we have begun this investigation. Future studies will aim at restoring upstream coupling to agonist and at defining the endogenous downstream target for GTPγS and subsequent elements that mediate actin polymerization.

We are grateful for excellent technical assistance from Alexandra Kudrjavcev-DeMilner, Hai Sun, and Julien Lartique. We are most grateful to Drs. K. Zhou and U. Knaus (The Scripps Research Institute) for purified PAK fragment and BV Cdc42, respectively; Dr. J. Meinkoth (University of Pennsylvania Medical School) for *E. coli*-expressed Cdc42; Drs. R. Cerione, T. Nomanbhoy, and J. Glaven (Cornell University) for recombinant Cdc24 and Dbl expressed in baculovirus; Dr. L. Tilney, and Pat Connelly (University of Pennsylvania) for help with EM; and Drs. S. Rittenhouse (Jefferson University Medical School), H. Goldfine, and B. Wolf (University of Pennsylvania Medical School) for help with the phospholipid synthesis.

National Institues of Health grants AI19883 to S.H. Zigmond; GM44428 to G.M. Bokoch; and GM28007 to P.N. Devreotes.

Received for publication 7 February 1997 and in revised form 18 April 1997.

References

Abo, A., M.R. Webb, A. Grogan, and A.W. Segal. 1994. Activation of NADPH oxidase involves the dissociation of p21rac from its inhibitory GDP/GTP exchange protein (rhoGDI) followed by its translocation to the plasma membrane. *Biochem. J.* 298:585–591.

Barkalow, K.W., K.J. Witke, D.J. Kwiatkowshi, and J.H. Hartwig. 1996. Coordinated regulation of platelet actin filament barbed ends by gelsolin and capping protein. *J. Cell Biol.* 134:389–399.

Bengtsson, T., E. Sarndahl, O. Stendahl, and T. Andersson. 1990. Involvement of GTP-binding proteins in actin polymerization in human neutrophils. *Proc. Natl. Acad. Sci. USA*. 87:2921–2925.

Bokoch, G.M.S. 1994. Regulation of the human neutrophil NADPH oxidase by the Rac GTP-binding proteins. *Curr. Opin. Cell Biol.* 6:212–218.

Bokoch, G.M., B.P. Bohl, and T.-H. Chuang. 1994. Guanine nucleotide exchange regulates membrane translocation of Rac/Rho GTP-binding proteins. *J. Biol. Chem.* 269:31674–31679.

Burbelo, P.D., D. Drechsel, and A. Hall. 1995. A conserved binding motif defines numerous candidate target proteins for both Cdc42 and Rac GTPases. *J. Biol. Chem.* 270:29071–29074.

Cano, M., D.A. Lauffenburger, and S.H. Zigmond. 1991. Kinetic analysis of F-actin depolymerization in polymorphonuclear leukocyte lysates indicates that chemoattractant stimulation increases actin filament number without altering filament length distribution. *J. Cell Biol.* 115:677–687.

Cerione, R.A., and Y. Zheng. 1996. The Dbl family of oncogenes. *Curr. Opin. Cell Biol.* 8:216–222.

Chardin, P., S. Paris, B. Antonny, S. Robineau, S. Beraud-Dufour, C.L. Jackson, and M. Chabre. 1996. A human exchange factor for ARF contains Sec7- and pleckstrinhomology domains. *Nature (Lond.).* 384:481–484.

Chen, M.Y., P.N. Devreotes, and R.E. Gundersens. 1994. *J. Biol. Chem.* 269: 20925–20930.

Chrzanowska-Wodnicka, M., and K. Burridge. 1996. Rho-stimulated contractility drives the formation of stress fibers and focal adhesions. *J. Cell Biol.* 133: 1403–1416.

Chuang, T.-H., B.P. Bohl, and G.M. Bokoch. 1993. Biologically active lipids are regulators of rac-GDI complexation. *J. Biol. Chem.* 268:26206–26211.

Devreotes, P.N., and S.H. Zigmond. 1988. Chemotaxis in eukaryotic cells: a focus on leukocytes and *Dictyostelium*. *Annu. Rev. Cell Biol.* 4:649–686.

Devreotes, P., D. Fontana, P. Klein, J. Sherring, and A. Theibert. 1987. Transmembrane signaling in *Dictyostelium*. *Methods Cell Biol.* 28:299–331.

Downey, G.P., C.K. Chan, and S. Grinstein. 1989. Actin assembly in electropermeabilized neutrophils: role of G-proteins. *Biochem. Biophys. Res. Commun.* 164:700–705.

Eaton, S., R. Wepf, and K. Simons. 1996. Roles for Racl and Cdc42 in planar polarization and hair outgrowth in the wing of *Drosophila*. *J. Cell Biol.* 135: 1277–1289.

Fukami, K., K. Matsuoka, O. Nakanishi, A. Yamakawa, S. Kawai, and T. Takenawa. 1988. Antibody to phosphatidylinositol 4,5-bisphosphate inhibits oncogene-induced mitogenesis. *Proc. Natl. Acad. Sci. USA*. 85:9057–9061.

Gilmore, A.P., and K. Burridge. 1996. Regulation of vinculin binding to talin and actin by phosphatidylinositol-4-5-bisphosphate. *Nature (Lond.).* 381: 531–535.

Hart, M.J., M.G. Callow, B. Souza, and P. Polakis. 1996. IQGAP1, a calmodulin-binding protein with a rasGAP-related domain, is a potential effector for Cdc42Hs. *EMBO (Eur. Mol. Biol. Organ.) J.* 15:2997–3005.

Hartwig, J.H., G.M. Bokoch, C.L. Carpenter, P.A. Janmey, L.A. Taylor, A. Toker, and T.P. Stossel. 1995. Thrombin receptor ligation and activated Rac uncap actin filament barbed ends through phosphoinositide synthesis in permeabilized human platelets. *Cell.* 82:643–653.

Heyworth, P.G., U.G. Knaus, X. Xu, D.J. Uhlinger, L. Conroy, G.M. Bokoch, and J.T. Curnutte. 1993. Requirement for postranslational processing of Rac GTP-binding proteins for activation of human neutrophil NADPH oxidase. *Mol. Biol. Cell.* 4:261–269.

Howard, T.H., and C.O. Oresajo. 1985. A method for quantifying F-actin in chemotactic peptide activated neutrophils: study of the effects of tBOC peptide. *Cell Motil.* 5:545–557.

Joneson, T., M. McDonough, D. Bar-Sagi, and L.V. Aelst. 1996. RAC regulation of actin polymerization and proliferation by a pathway distinct from Jun kinase. *Science (Wash. DC).* 274:1374–1376.

Kane, R.E. 1986. Components of the actin-based cytoskeleton. *In* Methods in Cell Biology. Academic Press, Inc., Orlando, FL. 229–242.

Kimura, K., and M. Ito. 1996. Regulation of myosin phosphatase by Rho and Rho-associated kinase (Rho-kinase). *Science (Wash. DC).* 273:245–248.

Knaus, U.G., P.G. Heyworth, B.T. Kinsella, J.T. Curnutte, and G.M. Bokoch. 1992. Purification and characterization of Rac 2: a cytosolic GTP-binding protein that regulates human neutrophil NADPH oxidase. *J. Biol. Chem.* 267:23575–23582.

Lamarche, N., N. Tapon, L. Stowers, P.D. Burbelo, P. Aspenstrom, T. Bridges, J. Chant, and A. Hall. 1996. Rac and Cdc42 induce actin polymerization and G_1 cell cycle progression independently of $p65^{pak}$ and the JNK/SAPK MAP kinase cascade. *Cell.* 87:519–529.

Laudanna, C., J.J. Campbell, and E.C. Butcher. 1996. Role of Rho in chemoattractant-activated leukocyte adhesion through integrins. *Science (Wash. DC).* 271:981–983.

Li, R., Y. Zheng, and D.G. Drubin. 1995. Regulation of cortical actin cytoskeleton assembly during polarized cell growth in budding yeast. *J. Cell Biol.* 128: 599–615.

Luo, L., Y.J. Liao, L.Y. Jan, and Y.N. Jan. 1994. Distinct morphogenetic functions of similar small GTPases: *Drosophila* Dracl is involved in axonal outgrowth and myoblast fusion. *Genes Dev.* 8:1787–1802.

Manser, E., T. Leung, H. Salihuddin, Z.-S. Zhao, and L. Lim. 1994. A brain serine/thrionine kinase activated by Cdc42 and Racl. *Nature (Lond.).* 367: 40–46.

McCallum, S.J., W.J. Wu, and R.A. Cerione. 1996. Identification of a putative effector for Cdc42Hs with high sequence similarity to the RasGAP-related protein IQGApl and a Cdc42Hs binding partner with similarity to IQGAP2. *J. Biol. Chem.* 271:21732–21737.

McRobbie, S.J., and P.C. Newell. 1983. Changes in actin associated with the cytoskeleton following chemotactic stimulation of *Dictyostelium discoideum*. *Biochem. Biophys. Res. Commun.* 115:351–359.

Moritz, A., J. Westerman, P.N.E.D. Graan, and K.W.A. Wirtz. 1992. Phosphatidylinositol 4-kinase and phosphatidylinositol-4-phosphate 5-kinase from bovine brain membranes. *Methods Enzymol.* 209:202–210.

Newell, P.C., G.N. Europe-Finner, G. Liu, B. Gammon, and C.A. Wood. 1990. Signal transduction for chemotaxis in *Dictyostelium* amoeba. *Semin. Cell Biol.* 1:105–113.

Nobes, C.D., and A. Hall. 1995. Rho, Rac, and Cdc42 GTPases regulate the assembly of multimolecular focal complexes associated with actin stress fibers, lamellipodia, and filopodia. *Cell.* 81:53–62.

Nobes, C.D., P. Hawkins, L. Stevens, and A. Hall. 1995. Activation of the small GTP-binding proteins rho and rac by growth factor receptors. *J. Cell Science.* 108:225–233.

Phillips, M.R., A. Feoktistov, M.H. Pillinger, and S.B. Abramson. 1995. Translocation of p21rac2 from cytosol to plasma membrane is neither necessary nor sufficient for neutrophil NADPH oxidase activity. *J. Biol. Chem.* 270: 11514–11521.

Redmond, T., M. Tardif, and S.H. Zigmond. 1994. Induction of actin polymerization in permeabilized neutrophils: role of ATP. *J. Biol. Chem.* 269:21657–21663.

Reif, K., C.D. Nobes, G. Thomas, A. Hall, and D.A. Cantrell. 1996. Phosphatidylinositol 3-kinase signals activate a selective subset of Rac/Rho-dependent effector pathways. *Curr. Biol.* 6:1445–1455.

Schafer, D.A., and J.A. Cooper. 1995. Control of actin assembly at filament ends. *Annu. Rev. Cell Dev. Biol.* 11:497–518.
Schafer, D.A., P.B. Jennings, and J.A. Cooper. 1996. Dynamics of capping protein and actin assembly in vitro: uncapping barbed ends by polyphosphoinositides. *J. Cell Biol.* 135:169–179.
Sells, M.A., U.G. Knaus, S. Bagrodia, D.M. Ambrose, G.M. Bokoch, and J. Chernoff. 1997. Human p21-activated kinase (Pakl) regulates actin organization in mammalian cells. *Curr. Biol.* 7:202–210.
Tardif, M., S. Huang, T. Redmond, D. Safer, M. Pring, and S.H. Zigmond. 1995. Actin polymerization induced by GTPγS in permeabilized neutrophils is induced and maintained by free barbed ends. *J. Biol. Chem.* 270:28075–28083.
Terui, T., R.A. Kahn, and P.A. Randazzo. 1994. Effects of acid phospholipids on nucleotide exchange properties of ADP-ribosylation factor 1. *J. Biol. Chem.* 269:28130–28135.
Therrien, S., and P.H. Naccache. 1989. Guanine nucleotide-induced polymerization of actin in electropermeabilized human neutrophils. *J. Cell Biol.* 109: 1125–1132.
Tolias, K.F., L.C. Cantley, and C.L. Carpenter. 1995. Rho family GTPases bind to phosphoinositide kinases. *J. Biol. Chem.* 270:17656–17659.
VanAeist, L., T. Joneson, and D. Bar-Sagi. 1996. Identification of a novel Racl-interacting protein involved in membrane ruffling. *EMBO (Eur. Mol. Biol. Organ.) J.* 15:3778–3786.
Whitehead, I., J. Kirk, and R. Kay. 1995*a*. Retroviral transduction and oncogenic selection of cDNA encoding Dbs, a homolog of the Dbl guanine nucleotide exchange factor. *Oncogene.* 10:713–721.
Whitehead, I., H. Kirk, C. Tognon, G. Trigo-Gonzales, and R. Kay. 1995*b*. Expression cloning of lfc, a novel oncogene with structual similarities to guanine nucleotide exchange factors and to regulatory region of protein kinase C. *J. Biol. Chem.* 270:18388–18395.
Wu, L., R. Valkema, P.J.M.V. Haastert, and P.N. Devreotes. 1995. The G protein β subunit is essential for multiple responses to chemoattractants in *Dictyostelium. J. Cell Biol.* 129:1667–1675.
Xu, X., D.C. Barry, J. Settleman, M.A. Schwartz, and G.M. Bokoch. 1994. Differing structural requirements for GTPase-activating protein responsiveness and NADPH oxidase activation by Rac. *J. Biol. Chem.* 269:23569–23574.
Zheng, Y., S. Bagrodia, and R.A. Cerione. 1994. Activation of phosphoinositide 3-kinase activity by Cdc42Hs binding to p85. *J. Biol. Chem.* 269:18727–18730.
Zheng, Y., J.A. Glaven, W.J. Wu, and R.A. Cerione. 1996. Phosphatidylinositol 4,5-bisphosphate provides an alternative to guanine nucleotide exchange factors by stimulating the dissociation of GDP from Cdc42Hs. *J. Biol. Chem.* 271:23815–23819.